

## On the determination of mass transfer in a concentration boundary layer

Gregory N. Nishihara<sup>1</sup> and Josef D. Ackerman<sup>1,2</sup>

<sup>1</sup>Department of Integrative Biology and <sup>2</sup>Faculty of Environmental Sciences, University of Guelph, Guelph, Ontario, N1G 2W1, Canada

### Abstract

The mass transfer of scalar quantities (e.g., O<sub>2</sub> and nutrients) in aquatic environments is an important and complex process involving diffusion and advection. In a flowing environment, concentration boundary layers (CBL) occur above the surfaces of organisms when they are a sink or source of scalars. In this study, we used an O<sub>2</sub> microsensor to profile the O<sub>2</sub> concentrations in the CBL above photosynthesizing freshwater macrophyte (*Vallisneria americana*) leaves that were oriented parallel to the flow in a recirculating flow chamber at 0.5 and 3.3 cm s<sup>-1</sup>. Measured O<sub>2</sub> profiles were nonlinear indicating the effect of higher order processes near the surface. O<sub>2</sub> flux ( $J_{obs}$ ) was estimated from these profiles by two nonlinear techniques, hyperbolic tangent and logarithmic models, and the commonly applied linear model. An integrated measurement of O<sub>2</sub> flux ( $J_{int}$ ) for each leaf was also measured independently in a stirred chamber. Whereas  $J_{obs}$  determined from the hyperbolic tangent ( $0.42 \pm 0.04$  [mean SE]  $\mu\text{mol m}^{-2} \text{s}^{-1}$ ) and linear ( $0.31 \pm 0.04 \mu\text{mol m}^{-2} \text{s}^{-1}$ ) models overestimated and underestimated  $J_{int}$  ( $0.37 \pm 0.05 \mu\text{mol m}^{-2} \text{s}^{-1}$ ), respectively, and were not velocity dependant, the hyperbolic tangent model provided the best fit ( $r^2 = 0.88$ ) compared with the linear model ( $r^2 = 0.77$ ). In addition, the slope of the regression against  $J_{int}$  ( $1.08 \pm 0.06$ ) was closest to 1.00 (i.e., a “perfect” fit). The logarithmic model varied with velocity and overestimated  $J_{obs}$  ( $0.98 \pm 0.22 \mu\text{mol m}^{-2} \text{s}^{-1}$  at  $0.005 \text{ m s}^{-1}$  and  $0.90 \pm 0.18 \mu\text{mol m}^{-2} \text{s}^{-1}$  at  $0.033 \text{ m s}^{-1}$ ). These results were confirmed in an analysis of 21 published O<sub>2</sub> concentration profiles measured next to sediments, microbial biofilms, planktonic algae, and epilithic algae. We would, therefore, recommend the hyperbolic tangent model to estimate mass transfer in a CBL.

The mass transfer of scalar quantities (i.e., dissolved gases, nutrients, and other chemicals) is an essential process for aquatic organisms (Jørgensen and Des Marais 1990, Falter et al. 2004, Larned et al. 2004). It is also a complex process that occurs through diffusion and advection, which, in turn, is a function of the state and flow characteristics of water, the physical and biological characteristics of organisms, the concentration of the scalar, and its molecular diffusivity (Sanford and Crawford 2000, Basmadjian 2003, Lorke et al. 2003). In stagnant water, diffusive flux ( $J_{diff}$ ) occurs, leading to the steady-state one-dimensional version of Fick’s first law of dif-

fusion, in which  $J_{diff}$  (defined here as positive for production and negative for uptake at the surface) is described by

$$J_{diff} = -D \frac{\partial C}{\partial z} \quad (1)$$

where  $D$  is the molecular diffusivity of the scalar, and  $\frac{\partial C}{\partial z}$  is the gradient in concentration ( $C$ ) of the scalar with distance ( $z$ ) from the surface. In a differential element near the surface of an aquatic organism, the unsteady one-dimensional equation that describes the distribution of a scalar concentration (e.g., O<sub>2</sub>) is

$$\frac{\partial C}{\partial t} = \frac{\partial}{\partial z} \left( D \frac{\partial C}{\partial z} \right). \quad (2)$$

Water flowing over the surface of the organism induces an advective flux ( $J_{adv}$ ) and can increase or decrease rates of physiological activity (Wheeler 1980, Jørgensen and Des Marais 1990, Stewart and Carpenter 2003). Far from the surface, momentum and mass transfer are dominated by inertial forces and the turbulent transport of momentum and scalar quanti-

\*Corresponding author. Phone: (519) 824-4120 ext. 54809; E-mail: ackerman@uoguelph.ca

### Acknowledgments

The authors would like to thank Bill Morton, Steve Wilson, and Ian Renaud for assistance with the mechanics and electronics of the equipment. This research was supported in part by funding from the University of Guelph and the Natural Sciences and Engineering Research Council of Canada to J.D.A.

ties are characterized by the eddy diffusivity of momentum ( $K_v$ ) and the eddy diffusivity of the scalar ( $K_D$ ), respectively. However, turbulence, in the case of  $K_v$ , is dissipated approaching the surface, where the dissipation rate is proportional to some function of  $z^3$  (Lin et al. 1953, Dade 1993, Bird et al. 2002), and near the surface of the organism viscous forces begin to dominate (Bird et al. 2002, Hondzo et al. 2005). The water velocity at the surface is at rest, due to the no-slip condition, and a velocity gradient between the surface and the free stream velocity ( $U$ ) forms a momentum boundary layer (BL).

As the momentum BL develops over a flat surface, a local Reynolds number ( $Re_x = Ux/\nu$ , at some distance ( $x$ ) downstream from the leading edge ( $\nu$  is the momentum diffusivity or the kinematic viscosity), can be used to characterize the nature of the momentum BL in the streamwise direction. The momentum BL is laminar nearest to the leading edge where  $Re_x < 2 \times 10^5$  (for a flat plate) and at higher  $Re_x$  further downstream, the BL becomes transitional and then turbulent when  $Re_x >$  the critical  $Re_x$  (i.e.,  $3\text{--}5 \times 10^5$  for a flat plate). A turbulent BL has vertical structure that can be separated into three regions: the outer layer, the logarithmic layer, and the viscous sublayer (VSL) adjacent to the surface (Schlichting and Gersten 2000). Therefore, the velocity profiles in the momentum BL gradually change in shape in the downstream direction from a laminar profile, where viscous forces are important throughout the BL, through a transitional profile, and finally to a fully turbulent profile, where viscous forces are most important in the VSL. The thickness of the VSL (i.e., of order,  $O[10^{-3}$  m]; Dade 1993) can be defined as the distance where the  $K_v$  and  $\nu$  are equal and is a region where the velocity gradient is linear near the surface (Tennekes and Lumley 1972).

It has been often convenient to define a relatively thin sublayer within the VSL, as the diffusive sublayer (DSL), also referred to as the diffusive boundary layer (DBL), where molecular diffusion ( $D$ ) is dominant (i.e., DSL thickness  $\sim O(10^{-4}$  m); Dade 1993). However, this simplification, which was developed as an analogy for heat transfer (Levich 1962), can be confusing since DBLs are typically defined by the momentum BL rather than through measurements of the distribution of scalar quantities (Hondzo et al. 2005). By analogy, a concentration boundary layer (CBL) forms when there is a concentration gradient between the surface of the organism (which is a source or a sink of the scalar) and the bulk water (Lin et al. 1953, Kader 1981). It is relevant to note that a CBL can exist in stagnant water for time periods less than the time necessary for diffusion to eliminate the gradient. In flowing conditions when the surface is a sink, the CBL often resembles the momentum BL. However, in aquatic environments, the Schmidt numbers ( $Sc = \nu/D$ ) are much greater than one, and so the shape of the momentum BL and CBL do not coincide close to the surface. Therefore, even though  $K_v$  is dampened by  $\nu$  in the VSL,  $K_v$  can still influence scalar distributions near the surface because  $K_v \approx K_D > D$  (Lin et al. 1953, Bird et al. 2002, Hondzo et al. 2005). Thus, due to the influence of the momentum BL, the CBL can also take on some

horizontal and vertical structure (Schlichting and Gersten 2000, Bird et al. 2002).  $D$  is important throughout a laminar CBL. However, within a fully turbulent CBL, three regions can be recognized (Lin et al. 1953, Kader 1981, Hondzo et al. 2005): (1) an outer region, where  $K_D \approx K_v > D$  and the concentration gradient is very small (i.e.,  $<1\%$ ); (2) a region where the concentration gradient increases exponentially,  $K_D$  decreases and  $D$  becomes more relevant with decreasing distance; and (3) the DSL of the CBL adjacent to the surface where the concentration gradient is the largest and where  $K_D \approx K_v < D$ .

The distribution of a scalar concentration in a differential element of the CBL can be described with respect to velocities ( $u$  in the  $x$  direction and  $w$  in the  $z$  direction) in two-dimensions at steady state (Levich 1962) by

$$u \frac{\partial C}{\partial x} + w \frac{\partial C}{\partial z} = \frac{\partial}{\partial z} \left( (D + K_D) \frac{\partial C}{\partial z} \right) \quad (3)$$

where the left-hand side of the equation describes the advective flux ( $J_{adv}$ ) and the right-hand side describes  $J_{diff}$  and the flux due to turbulent diffusion. The appearance of the velocity terms and  $K_D$  in Eq. 3 shows the dependence of the scalar concentration on the momentum BL. The relative importance of these terms remains to be determined; however, the effects of  $K_D$  are transmitted to the surface (Shaw and Hanratty 1977, Bird et al. 2002) and can affect mass transfer throughout the CBL.

There are two methods for estimating mass transfer: (1) mechanistic models such as those from Dade (1993) and Thomas and Atkinson (1997) that require additional information on the characteristics of flow and the surface being investigated and (2) empirically based models of the scalar concentration gradient measured directly using microsensors. Typically mass transfer determined from concentration profiles assume linear concentration gradients (i.e., Eq. 1) (Crank 1977) neglecting the effects of nonlinear terms (Jørgensen and Des Marais 1990, Lorenzen et al. 1995, Larkum et al. 2003). Alternatively, Lewandowski et al. (1993) fit a logarithmic model to the concentration profile to estimate flux; more recently, a mechanistic model incorporating a power-law function was proposed to describe the  $O_2$  profile above sediments (Hondzo et al. 2005). Other empirical equations have long been used to model asymptotic data (Jassby and Platt 1975) among which a hyperbolic tangent was found most appropriate. Clearly, a more detailed treatment of these approaches is needed. This report will, therefore, examine and compare methods used to estimate the flux from CBL profiles by measuring the concentration of  $O_2$  next to the freshwater macrophyte, *Vallisneria americana* Michx.

## Materials and procedures

*Experimental apparatus*—Experiments were conducted in a  $10 \times 10 \times 100$  cm long flume with flow straighteners in the first 12 cm. Flow rates were manipulated with a combination of a ball valve and a 5-cm gate near the exit, and the average velocities ( $U$ ) were determined from volumetric flow measurements.

The flow approaching the leading edge of the leaf was uniform and well behaved in the region where the leaves were placed (Nishihara and Ackerman 2006). Bulk water was recirculated by a submersible pump (3E-12N, Little Giant Pump Co.) from a 0.030 m<sup>3</sup> reservoir. Well-aerated tap water was used in all experiments to maintain O<sub>2</sub> and CO<sub>2</sub> saturation. The flume water temperature was kept at 24°C by placing the reservoir and pump in a constant temperature water bath. Bulk O<sub>2</sub> was measured with an OXN oxygen microsensors (Unisense).

An OX25 oxygen microsensors (Unisense) was attached to a motorized micromanipulator with a vertical resolution of 0.010 mm and positioned 2.5 cm from the leading edge of the leaf. Both O<sub>2</sub> microsensors were attached to a picoammeter (PA2000, Unisense) and the data were recorded to a computer via DAQ (PMD-1208LS, Measurement Computing). Motor control and data recording were accomplished with custom software (LabView 7.1, National Instruments). The bulk pH and temperature (AB15+, Fisher Science) were measured and recorded similarly. Photosynthetically active radiation (PAR) was provided by a slide projector equipped with an 82V 300W lamp (General Electric). PAR in the region of testing was 153 μmol photon m<sup>-2</sup> s<sup>-1</sup> as measured with a 4π sensor (QSL2101, Biospherical Instruments), which was sufficient to saturate photosynthesis in this system.

Leaves used in the experiments were carefully selected to have no visible epiphytes and no undulations. The flat sections were cut from the middle third of the leaf and were 0.9 ± 0.04 cm (average ± SE) wide and at least 7.0 cm long. Selected leaves were allowed to acclimate in a 24°C water bath overnight prior to experiments. The leaf sections were attached to a 3.0 cm tall wire stand with cyanoacrylate-based glue and placed in the working section of the flume 56 cm downstream of the flow straighteners, perpendicular to the light source and parallel to the flow.

No changes in O<sub>2</sub> concentration in the bulk water were observed during experiments, therefore the O<sub>2</sub> measured during profiling were converted to % O<sub>2</sub> saturation by dividing the measured voltage by the voltage obtained when the microsensors was farthest from the leaf surface and in the bulk fluid. The % O<sub>2</sub> saturation was converted to molar concentration (263 mmol m<sup>-3</sup>) by multiplying by the O<sub>2</sub> saturation concentration of oxygen in freshwater at 24°C.

**Data analysis: Hyperbolic tangent model**—The observed O<sub>2</sub> flux ( $J_{obs}$ ) from a photosynthesizing leaf can be estimated from the O<sub>2</sub> profile as O<sub>2</sub> is transported from the leaf surface by the flowing water. In an ideal case, the O<sub>2</sub> CBL is described by Eq. 3 by first examining the conditions when  $J_{adv}$  is zero, i.e., at the surface where the velocity and  $K_D$  are zero. The  $J_{obs}$  from the leaf is then estimated by Fick's first law at the leaf surface,

$$J_{obs} = -D \left. \frac{dC}{dz} \right|_{z=0} \quad (4)$$

As mentioned previously, this simplification is often applied and the flux is determined by assuming a linear gradi-

ent in the lower portion of the CBL or by, more recently, fitting a logarithmic function to the dimensionless concentration gradient (see below). Alternatively,  $J_{obs}$  can be determined by nondimensionalizing the O<sub>2</sub> concentration evaluated at the surface ( $C_s$ ) and the bulk water ( $C_b$ ) and fitting a hyperbolic tangent to the dimensionless concentration gradient ( $\theta$ ). The hyperbolic tangent is an appropriate empirical model to describe the O<sub>2</sub> concentration profile because for large  $z$ , the derivative of the function approaches 0 (i.e., no concentration gradient) and for  $z$  very near the surface, the derivative is almost constant (i.e.,  $K_D \ll D$  and  $u$  approaches 0, describing the case where mass transfer is diffusion controlled). This dimensionless concentration gradient is given by,

$$\theta = \frac{C - C_s}{C_b - C_s} \quad (5)$$

where the local values,  $\theta(z)$ , can be modeled as,

$$\theta(z) = B \tanh\left(\frac{A}{B}z\right) \quad (6)$$

where  $A$  is a constant that describes the slope at  $z = 0$  and  $B$  is a constant that describes the value of the asymptote. In this case,

$$\frac{d\theta}{dz} = A \left(1 - \tanh^2\left(\frac{A}{B}z\right)\right) \quad (7)$$

and when Eq. 7 is evaluated at  $z = 0$ ,

$$\left. \frac{d\theta}{dz} \right|_{z=0} = A \quad (8)$$

Since,

$$\left. \frac{dC}{dz} \right|_{z=0} = A(C_b - C_s) \quad (9)$$

the O<sub>2</sub> flux can be calculated as,

$$J_{obs} = -DA(C_b - C_s) \quad (10)$$

**Linear and logarithmic models**—In the case of a linear model used to estimate  $J_{obs}$ , Fick's law is assumed to be valid for some distance into the CBL and can be calculated from the slope of the line that best describes the most linear portion of the O<sub>2</sub> distribution (Crank 1977),

$$J_{obs} = -D \frac{\Delta C}{\Delta z} \quad (11)$$

where  $\Delta$  is the difference operator. For cases where a logarithmic profile is assumed, Fick's law only applies at  $z = 0$ , since advection is expected to influence mass flux where velocities are not zero. The profile is nondimensionalized (Eq. 6) and the slope ( $m$ ) of the linearized distribution is calculated,

$$\ln(1 - \theta) = mz \quad (12)$$

The derivation of the concentration gradient is similar to that of Eq. 10, where  $A$  is replaced by  $m$  (Lewandowski et al. 1993).

**O<sub>2</sub> flux calculation**—The O<sub>2</sub> profiles of 20 *V. americana* leaves were determined at  $U$  of 0.5 and 3.3 cm s<sup>-1</sup> ( $Re_x = 136$  and 895, respectively). O<sub>2</sub> profiles were measured by positioning the OX25 microsensor at the leaf surface while viewing through a dissecting microscope. O<sub>2</sub> concentrations were determined at  $z = 0.00$  to 0.10 mm in 0.02 mm steps, 0.10 to 0.50 mm in 0.10 mm steps, and at 0.75 and 1.00 mm for the first 12 leaves. The number of steps were increased for the remainder of the leaves, where  $z = 0.00$  to 0.20 mm in 0.02 mm steps, 0.10 to 1.00 mm in 0.10 mm steps, and at 2.00 and 3.00 mm. Data were recorded for 30 s at 5 Hz. The initial position,  $z = 0$ , was appropriately offset, before estimating  $J_{obs}$ , to accommodate the difficulty in positioning the microsensor tip precisely at the leaf surface. Improper positioning (i.e., when the tip was positioned below the plane of the leaf surface) was observed when there was no decrease in O<sub>2</sub> concentration as the microsensor was repositioned away from the leaf surface. Two profiles were determined at each  $U$  for each leaf, and  $J_{obs}$  was estimated from the profiles. Further analyses used the averaged  $J_{obs}$  from the two profiles, except in the case of leaf 1 and 3, where only one profile could be obtained.

An independent O<sub>2</sub> flux measurement for each leaf was also made in a stirred chamber following the flow chamber profiles. In this case, the integrated O<sub>2</sub> flux ( $J_{int}$ ) was determined by placing the leaf section in a 25 mL Erlenmeyer flask with a magnetic stir bar. Sections were glued on a glass frame made of capillary tubing to prevent the leaf from touching the sides of the flask and to ensure that the leaf was oriented perpendicular to the light source (153 μmol photon m<sup>-2</sup> s<sup>-1</sup>). Water was added to the flask by submersing the flask into the reservoir of the flume and capping it with a one-hole rubber stopper so that no bubbles remained in the flask. The flask was placed in a glass water bath, which was placed on a magnetic stirrer. The stirring rate was set to 400 rpm, water temperature was 24°C and the OXN oxygen microsensor was carefully inserted through the hole into the flask. Measurements taken at 4 Hz for 15 min showed a linear relationship, therefore  $J_{int}$  was calculated by the following equation:

$$J_{int} = \frac{C_t - C_0}{t - t_0} \times \frac{V}{S} \quad (13)$$

where  $C_0$  and  $C_t$  are the initial and final O<sub>2</sub> concentration, respectively,  $t_0$  and  $t$  are the initial and final time,  $V$  is the volume of the flask, and  $S$  is the surface area of both sides of the leaf. The test conditions in the stirred chamber were assumed to be above saturation for dissolved inorganic carbon (i.e., DIC ≥ 4.8 mol m<sup>-3</sup>).

**Examples from the literature**—An assessment of how the flux estimate varied by model applied was made by digitizing O<sub>2</sub> profiles from published literature using ImageJ (Abramoff et al. 2004). In figures where the data points were difficult to distinguish, the best effort was made to select the clearest data point and care was taken to prevent over-sampling, which would artificially increase the number of data points relative to the

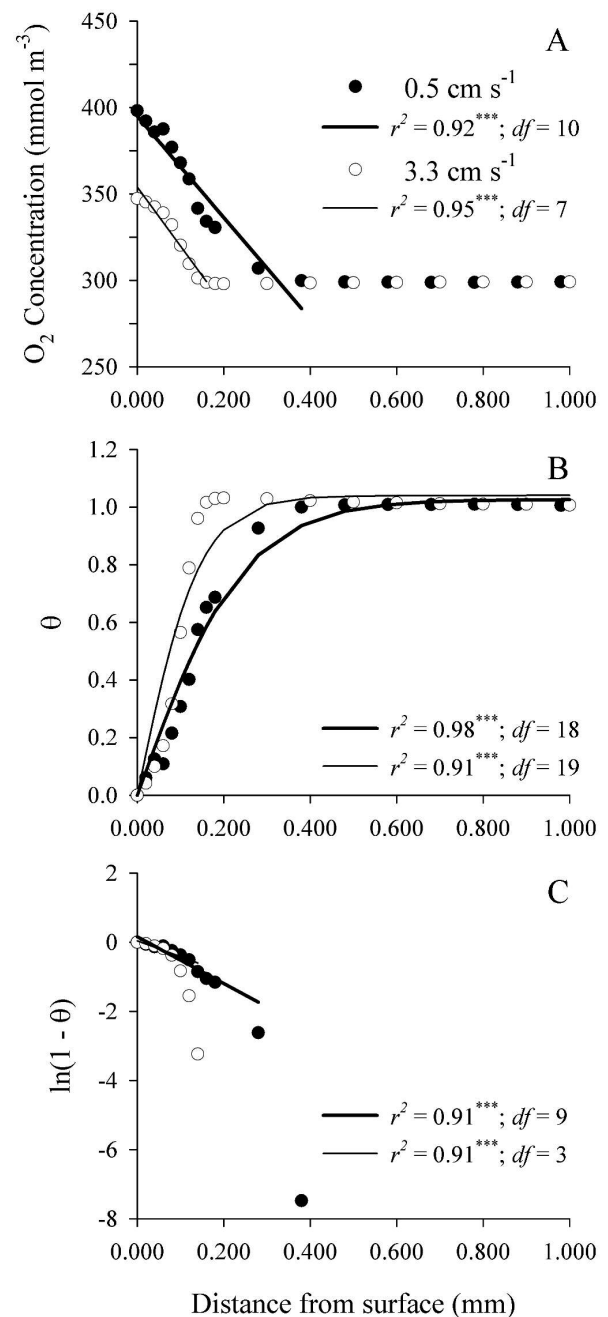


**Fig. 1.** An example of the O<sub>2</sub> concentration profile measured above a *Valisneria americana* leaf at 0.5 cm s<sup>-1</sup> (black dots) and 3.3 cm s<sup>-1</sup> (white dots). (A) O<sub>2</sub> concentration profile. (B) Dimensionless O<sub>2</sub> profile. (C) Natural log-transformed dimensionless O<sub>2</sub> profile. Lines are regressions to the plotted data. \*\*\* $P < 0.001$ .

original figure. The data points critical to this study (i.e., points near the surface) were well resolved in all the figures. Published studies were arbitrarily chosen to represent a range of ecological systems typically investigated with O<sub>2</sub> microsensors.

**Statistical analyses**—Data were analyzed using linear and nonlinear regressions with Statistica Release 6.1 (Statsoft, Inc.)

**Table 1.** A comparison of the models (hyperbolic tangent, linear, and logarithmic models) used to estimate the  $O_2$  gradient next to a *Vallisneria americana* leaf. Differences in the number of profiles analyzed are a result of profiles that did not have enough points to use in a regression. All regressions were significant ( $P < 0.05$ ).

$r^2$	Hyperbolic tangent		Linear		Logarithmic	
	0.5 cm s <sup>-1</sup>	3.3 cm s <sup>-1</sup>	0.5 cm s <sup>-1</sup>	3.3 cm s <sup>-1</sup>	0.5 cm s <sup>-1</sup>	3.3 cm s <sup>-1</sup>
Average	0.98	0.92	0.94	0.91	0.93	0.83
Standard error	< 0.001	< 0.001	< 0.001	< 0.001	< 0.001	< 0.001
Max. value	1.00	0.99	1.00	1.00	1.00	0.98
Min. value	0.95	0.50	0.79	0.59	0.76	0.33
Number of $r^2 > 0.900$	38	32	31	24	27	13
Number of $r^2$ from 0.800 ~ 0.900	0	4	6	6	10	10
Number of $r^2 < 0.800$	0	2	1	5	1	10
$n$	38	38	38	35	38	33

Differences in the number of profiles analyzed are a result of profiles that did not have enough points to use in a regression. All regressions were significant ( $p < 0.05$ ).

and Excel 2003 (Microsoft Corp.). The standard errors are reported after the averages, unless otherwise stated. Analysis of variance (ANOVA) was used to compare differences in the average  $r^2$  between low and high velocities within each model and analysis of covariance (ANCOVA) was used to determine whether there were any differences between the slopes within each model and  $U$ .

### Assessment

A typical  $O_2$  profile over a photosynthesizing leaf at 0.5 and 3.3 cm s<sup>-1</sup> shows the nonlinearity in the CBL < 0.100 mm from the leaf (Fig. 1A). As the microsensor was moved away from the surface, the  $O_2$  concentration decreased to a constant value in the bulk flow, where the concentration gradient was zero. The nonlinearity is more apparent at 0.5 cm s<sup>-1</sup>, where the decrease in the concentration gradient occurs more gradually with decreases in steepness between 0.200 and 0.500 mm. The differences in the concentration gradients at 0.5 cm s<sup>-1</sup> and 3.3 cm s<sup>-1</sup> are also evident in the dimensionless  $O_2$  profiles (Fig. 1B). The  $r^2$  of the hyperbolic tangent model used in Fig. 1B was 0.98 ( $df = 18$ ,  $P < 0.001$ ) at 0.5 cm s<sup>-1</sup> and 0.91 ( $df = 19$ ,  $P < 0.001$ ) at 3.3 cm s<sup>-1</sup>.

When a linear concentration gradient was assumed,  $O_2$  flux could be estimated from the most linear part of the  $O_2$  concentration gradient (i.e., within 0.200 and 0.100 mm of the surface at 0.5 cm s<sup>-1</sup> and 3.3 cm s<sup>-1</sup>, respectively; Fig. 1A). It was often difficult to choose the appropriate number of points to include in the analyses, due to the nonlinearity and the fact the results proved to be variable and dependent on the number of point chosen (see below). Therefore by convention, every effort was made to maximize the  $r^2$  of the linear regression and to use at least 5 points to determine the slope in a statistically rigorous manner. The  $r^2$  was 0.92 ( $df = 10$ ,  $P < 0.001$ ) at 0.5 cm s<sup>-1</sup> and 0.95 ( $df = 7$ ,  $P < 0.001$ ) at 3.3 cm s<sup>-1</sup> (Fig. 1A). Using the same convention, the slopes for the logarithmic model were estimated (Fig. 1C) and the  $r^2$  was 0.91 ( $df = 9$ ,  $P < 0.001$ ) at 0.5 cm s<sup>-1</sup> and 0.91 ( $df = 3$ ,  $P < 0.001$ ) at 3.3 cm s<sup>-1</sup>.

On average, the  $r^2$  of all models were higher for 0.5 cm s<sup>-1</sup> than at 3.3 cm s<sup>-1</sup>, probably due to the larger number of points that could be used in the regression. Of the 38 profiles analyzed, the  $r^2$  were highest for the hyperbolic tangent model of which only 6 regressions at 3.3 cm s<sup>-1</sup> were < 0.900 (Table 1). In contrast,  $J_{obs}$  could not be determined for 3 profiles in the linear and 5 profiles in the logarithmic models at 3.3 cm s<sup>-1</sup>. Moreover, compared to 6 hyperbolic tangent profiles, 18 of the linear, and 31 of the logarithmic profiles had  $r^2 < 0.900$ .

An assessment of the flux determined above using the hyperbolic tangent, linear, and logarithmic models was made by comparing  $J_{obs}$  to  $J_{int}$  from the stirred chamber (Fig. 2). In this case,  $J_{int}$  is considered to be an independent and integrated estimate of the “true”  $O_2$  flux at saturating conditions. Thus, a measure of the model’s accuracy can be evaluated by how close the slope of a regression of  $J_{obs}$  on  $J_{int}$  is to 1.00 (i.e., a “perfect” fit). The slopes for the hyperbolic tangent model were closer to 1.00 at both  $U$ , whereas the slopes of the linear model were lower and the slopes of the logarithmic model were higher (Table 2). An ANCOVA confirmed that there were significant differences among the slopes ( $F_{6, 107} = 99.86$ ,  $P < 0.001$ ), and only the  $y$ -intercept of the regression of the logarithmic model at 0.5 cm s<sup>-1</sup> was significantly different from zero.

There was no differences in the slopes among  $U$  for the hyperbolic tangent ( $F_{1, 36} = 0.453$ ,  $P = 0.51$ ) or linear ( $F_{1, 36} = 1.29$ ,  $P = 0.26$ ) models, but there were differences between  $U$  for the logarithmic model ( $F_{1, 35} = 5.60$ ,  $P < 0.05$ ) (Fig. 2). Given this result, an ANCOVA was used to determine whether there were differences between the hyperbolic tangent and linear models. In this analysis, the data for the two  $U$  were pooled for each model. The ANCOVA revealed that the slope of the hyperbolic tangent model ( $1.08 \pm 0.06$ ,  $r^2 = 0.88$ ,  $df = 38$ ,  $P < 0.01$ ) was significantly ( $F_{1, 76} = 5.62$ ,  $P < 0.05$ ) greater than that of the linear model ( $0.85 \pm 0.07$ ,  $r^2 = 0.77$ ,  $df = 38$ ,  $P < 0.01$ ). The lower predictions of  $J_{obs}$  by the linear model (slope always < 1.00) were likely due to differences in the nature of the regressions. Specifically, the hyperbolic tangent model measures the slope

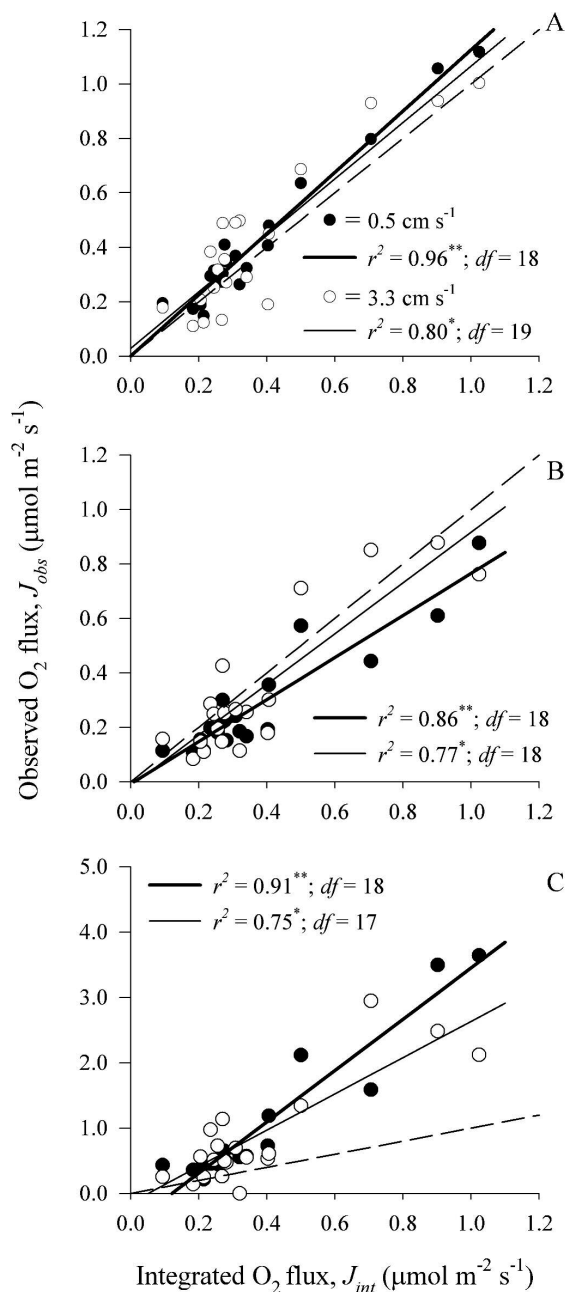


**Fig. 2.** The O<sub>2</sub> flux ( $J_{obs}$ ) above a *Vallisneria americana* leaf estimated from the hyperbolic tangent, linear, and logarithmic models at 0.5 cm s<sup>-1</sup> (black dots) and 3.3 cm s<sup>-1</sup> (white dots) compared with the integrated O<sub>2</sub> flux ( $J_{int}$ ) estimated independently in a stirred chamber. (A)  $J_{obs}$  estimated from the hyperbolic tangent model. (B)  $J_{obs}$  estimated from the linear model. (C)  $J_{obs}$  estimated from the logarithmic model. Solid lines are the regressions of  $J_{obs}$  on  $J_{int}$  and the dashed line indicates a slope of 1. Note the different range for the y-axis of Fig. 2C. \* $P < 0.05$  and \*\* $P < 0.01$ .

at  $z = 0$ , whereas the linear model integrates between  $z = 0$  and some distance,  $z_1$ , away from the surface where the points become nonlinear. Note that the application of Fick's law is valid at  $z = 0$ . The large slopes and poor relationship of  $J_{obs}$  to  $J_{int}$  described by the logarithmic fit is likely a result of the small

number of data points available to estimate O<sub>2</sub> flux. As mentioned above, the results were also quite variable when a small number of data points were used to estimate  $J_{obs}$ , and in the case of the linear model the  $J_{obs}$  to  $J_{int}$  slopes deviated greatly from 1.00 (e.g., slope = 15.6 and 16.6 for the first 3 and 4 points near the leaf surface, respectively). Given that the slope of the regression of the hyperbolic tangent model on  $J_{int}$  was closest to 1.00 (which was also within the 95% confidence interval of the slope of the hyperbolic tangent model) and had the higher  $r^2$ , the hyperbolic tangent model appears to provide the better estimate of  $J_{obs}$ .

The difference in  $J_{obs}$  estimated from each model is evident using the example presented in Fig. 1 where  $J_{int}$  was 0.88 μmol m<sup>-2</sup> s<sup>-1</sup> (Table 3). In this case, the hyperbolic tangent model provided estimates that were closest to  $J_{int}$  (i.e., within 6 to 12%). In contrast, the linear model provided estimates of  $J_{obs}$  that were within 7% and 20% of  $J_{int}$ , whereas the logarithmic model provided the poorest estimates of  $J_{int}$  (i.e., within 42% to 81%). These results were also evident in the larger data set averaging the 20 leaves (Table 4). The average  $J_{obs}$  of the 20 leaves determined from the hyperbolic tangent model ( $0.42 \pm 0.04$  μmol m<sup>-2</sup> s<sup>-1</sup>) was again closest to  $J_{int}$  ( $0.37 \pm 0.05$  μmol m<sup>-2</sup> s<sup>-1</sup>),  $J_{obs}$  for the linear model was lower ( $0.31 \pm 0.04$  μmol m<sup>-2</sup> s<sup>-1</sup>), and the logarithmic model overestimated  $J_{obs}$  ( $0.94 \pm 0.14$  μmol m<sup>-2</sup> s<sup>-1</sup>).

To further assess the utility of the hyperbolic tangent model, the characteristics of O<sub>2</sub> flux (uptake or production) were examined in a variety of ecological systems: sediments (Glud et al. 1994), biofilms (Jørgensen and Des Marais 1990, Lewandowski et al. 1993); epilithic algae (Larkum et al. 2003), and planktonic algae (Ploug et al. 1999) (See [Web appendix A](#)). Visual inspection of the published figures indicated nonlinearity in the O<sub>2</sub> profiles, hence supporting the comparison. Since the O<sub>2</sub> flux from these systems were not verified independently (e.g., using a stirred chamber measurement), the flux estimated from the linear and logarithmic models were compared against the hyperbolic tangent model (Fig. 3). As observed for  $J_{obs}$  from *V. americana*, the linear model underestimated  $J_{obs}$  - hyperbolic tangent (slope =  $0.77 \pm 0.02$ ), and the logarithmic model was more variable and overestimated  $J_{obs}$  - hyperbolic tangent (slope =  $1.3 \pm 0.1$ ) (Fig. 3 and 4). Moreover, a greater number of data points could be included in the analysis for the hyperbolic tangent model, in contrast to the linear and logarithmic models (Appendix A). The  $r^2$  of the regressions of all the models were  $> 0.91$ , which is not surprising since the  $r^2$  of the linear and logarithmic models were maximized (See [Web appendix A](#)) as described above.

## Discussion

It is apparent from the results that a hyperbolic tangent model provides the best estimates of the O<sub>2</sub> flux for *V. americana* leaves that closely match an independent technique (e.g., a stirred chamber measurement). Differences among models used to determine flux likely exist because the linear model

**Table 2.** Linear regression statistics for Fig. 2 of the  $O_2$  flux ( $J_{obs}$ ) estimated from the concentration boundary layer next to *Vallisneria americana* leaves using the hyperbolic tangent, linear, and logarithmic models compared to an integrative measurement in a stirred chamber ( $J_{int}$ ). Note that the logarithmic model could not be applied to the data from one leaf used in the analysis at  $3.3 \text{ cm s}^{-1}$ .

Model	Velocity ( $\text{cm s}^{-1}$ )	Slope $\pm \text{SE}$	Intercept $\pm \text{SE}$	$r^2$	df	$p$
Hyperbolic tangent	0.5	$1.12 \pm 0.05$	$0.000001 \pm 0.00002$	0.96	18	<0.01
	3.3	$1.04 \pm 0.12$	$0.000029 \pm 0.00005$	0.80	18	<0.05
Linear	0.5	$0.77 \pm 0.07$	$-0.000007 \pm 0.00003$	0.85	18	<0.01
	3.3	$0.93 \pm 0.12$	$-0.000015 \pm 0.00005$	0.76	18	<0.05
Logarithmic	0.5	$3.92 \pm 0.30$	$-0.000474 \pm 0.00013$	0.90	18	<0.01
	3.3	$2.78 \pm 0.39$	$-0.000142 \pm 0.00017$	0.74	17	<0.05

ignores the effects of higher order processes (e.g., advection,  $K_D$ , and reactions) adjacent to the surface and the logarithmic model is subject to low degrees of freedom in the fit of the model. These patterns were also observed in an evaluation of studies involving a range of ecological systems (sediments [Glud et al. 1994], biofilms [Jørgensen and Des Marais 1990, Lewandowski et al. 1993], epilithic algae [Larkum et al. 2003], and planktonic algae [Ploug et al. 1999]). Importantly, the data presented in these studies clearly indicates that the CBLs were nonlinear (e.g., Ploug et al. 1999 and Jørgensen and Des Marais 1990). This suggests that there are insufficient data points available to make good estimates of  $O_2$  flux from a linear model (e.g., Ploug et al. 1999). It is relevant to note that the DSL thickness is predicted to be relatively thin (i.e.,  $O$  [ $10^{-3}$  to  $10^{-4}$  m], Dade 1993); however, recent data demonstrates the actual thickness is much lower and on the order of  $10^{-5}$  m as described in Nishihara and Ackerman (2006). This realization would limit the effectiveness of linear regression techniques to less than 0.100 mm of the surface at the relatively low velocities used in this study. The spatial resolution would likely be smaller at higher velocities.

Recently, a mechanistic model based on a power-law formulation was proposed by Hondzo et al. (2005) as an improvement over the linear approximations used to describe the concentration gradient adjacent to a surface because the new model attempts to address the effects of  $K_D$  on  $O_2$  mass transfer in a turbulent BL. Analogous to the power-law scaling of a turbulent momentum BL, their formulation assumes a linear concentration profile in the DSL and a logarithmic distribution otherwise and describes  $O_2$  profile over a sediment bed. However, the universality of the model remains to be determined, since the model does not consider chemical (e.g.,  $\text{HCO}_3^-$  and  $\text{CO}_2$  chemistry in the CBL adjacent to photosynthesizing aquatic plants) and biological processes (e.g., nonlinear or Michaelis-Menten type reactions that affect the flux of scalar quantities through a surface) that may affect concentration profiles in biologically and chemically active living systems (Dang 1983, Bird et al. 2002, Nishihara and Ackerman 2006). It is beyond the scope of this study to present a mechanistic model that incorporates such processes. Nevertheless, the empirical model proposed in this study, which does not

assume linear concentration gradients throughout the CBL, was effective in estimating  $O_2$  flux from measured  $O_2$  profiles above photosynthesizing *V. americana* leaves, which were comparable to integrative estimates of  $O_2$  flux measured in a stirred chamber.

Equation 3 predicts the nonlinearity of the concentration profiles, as observed in the  $O_2$  profiles determined in this and past studies. Physical, chemical, and biological processes affect CBLs and cause deviations from the underlying assumptions of a linear concentration gradient required to estimate flux (Cussler 1997). For example, in porous surfaces such as sediments, biofilms, and epiphytes, some advection occurs at the surface and within their structures (Rasmussen and Lewandowski 1998), requiring estimates of  $u$  and  $w$  at the surface, which can be difficult to obtain. Microsensors are also thought to affect the momentum BL and change the characteristics of the  $O_2$  profile, which may lead to underestimates at  $u < 1 \text{ cm s}^{-1}$  and overestimates at  $u > 1 \text{ cm s}^{-1}$  (Glud et al. 1994, Rasmussen and Lewandowski 1998); however, this effect was considered minimal over the surface of a sediment (Hondzo et al. 2005). Moreover, in aquatic environments, where Schmidt numbers are large, mass transport associated with  $K_D$  influences concentration distributions closer to the surface of an organism because the distribution of scalar concentrations are associated with the Batchelor microscale in contrast to the Kolmogorov microscale used for momentum (Moore and Crimaldi 2004). It is relevant to note that the analogy between momentum and scalar transport was found to be poor near surfaces and evidence suggests that in the DSL,  $K_v \neq K_D$  (Shaw

**Table 3.** The  $O_2$  flux ( $J_{obs}$ ) estimated from the concentration boundary layer next to the *Vallisneria americana* leaf in Fig. 1 using the hyperbolic tangent, linear, and logarithmic models compared to an integrative measurement in a stirred chamber ( $J_{int}$ ).

	$J_{obs}$ ( $\mu\text{mol m}^{-2} \text{s}^{-1}$ )		
	Hyperbolic Tangent	Linear	Logarithmic
$0.5 \text{ cm s}^{-1}$	0.98	0.70	1.60
$3.3 \text{ cm s}^{-1}$	0.82	0.82	0.51
	$J_{int} = 0.88$		

**Table 4.** The  $O_2$  flux ( $J_{obs}$ ) estimated from the concentration boundary layer next to *Vallisneria americana* leaves ( $n = 20$ ) using the hyperbolic tangent, linear, and logarithmic models compared to an integrative measurement in a stirred chamber ( $J_{int}$ ).

	$J_{obs}$ ( $\mu\text{mol m}^{-2} \text{s}^{-1}$ )		
	Hyperbolic Tangent	Linear	Logarithmic
0.5 $\text{cm s}^{-1}$	$0.42 \pm 0.06$	$0.28 \pm 0.04$	$0.98 \pm 0.22$
3.3 $\text{cm s}^{-1}$	$0.41 \pm 0.06$	$0.33 \pm 0.06$	$0.90 \pm 0.18$
Average $\pm$ SE	$0.42 \pm 0.04$	$0.31 \pm 0.04$	$0.94 \pm 0.14$
	$J_{int} = 0.37 \pm 0.05$		

and Hanratty 1977, Na and Hanratty 2000). Moreover, biological and chemical reactions occurring in the DSL can also affect mass transfer by influencing the shape of the concentration gradient and may reduce or enhance mass transfer rates (Acrivos and Chambré 1957, Chambré and Young 1958, Mitrovic and Papavassiliou 2004). Thus adding a reaction term to Eq. 3 (e.g., physiological reactions under kinetic control or the chemistry of  $\text{HCO}_3^-$  and  $\text{CO}_2$  in the DSL of a photosynthesizing organism) and expressing  $K_D$  as a function of  $z$  may provide better theoretical estimates of mass transfer (Bird et al. 2002, Wolf-Gladrow and Riebesell 1997, Nishihara and Acker-

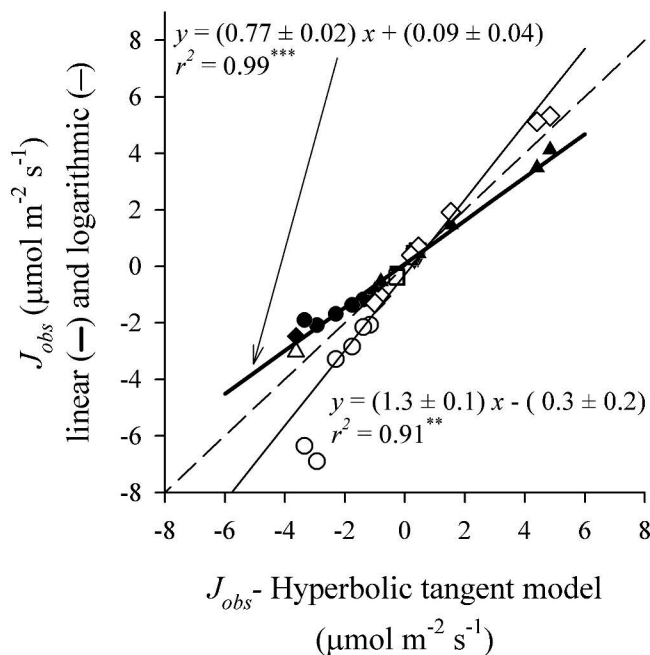


**Fig. 3.** The variation in  $O_2$  flux ( $J_{obs}$ ) above a variety of ecological surfaces estimated from the linear (black symbols) and logarithmic (white symbols) models compared with the hyperbolic tangent model. Symbols indicate different studies: Jørgensen and Des Marais 1990 (circles), Glud et al. 1994 (squares), Lewandowski et al. 1993 (diamond), Ploug et al. 1999 (inverted triangles), and Larkum et al. 2003 (triangles). Linear regressions show the slope and intercepts  $\pm$  standard deviation, and the dashed line indicates a slope of 1.  $**P < 0.01$  and  $***P < 0.001$ .

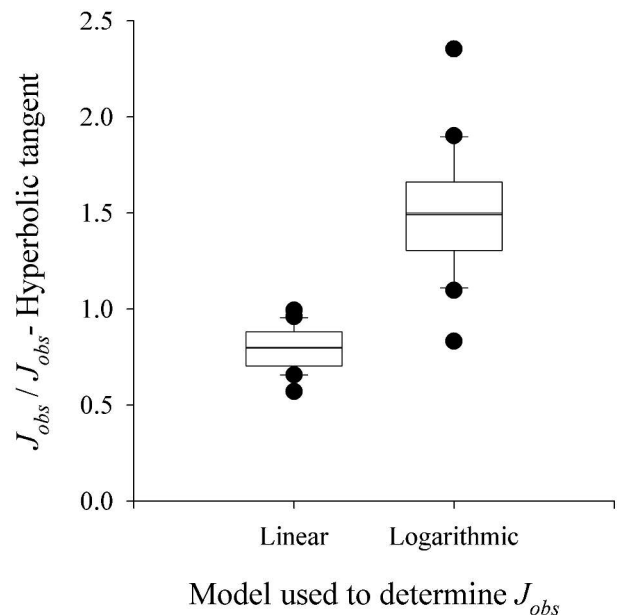


**Fig. 4.** The distribution of the ratios of  $O_2$  flux ( $J_{obs}$ ) estimated from the linear and logarithmic models compared with the hyperbolic tangent model of published studies showing the 10th, 25th, 75th, and 90th percentiles. The center line indicates the median and the black dots indicate outliers ( $n = 21$ ).

man 2006). It is unlikely that the relatively smooth surface of a *V. americana* leaf caused any nonlinearity in the  $O_2$  profile, however it is possible that metabolic processes influence  $O_2$  profiles above the leaf surface (Nishihara and Ackerman 2006). Regardless, the hyperbolic tangent model used in this study predicted  $J_{obs}$  determined using an independent method.

### Comments and recommendations

Ideally, the flux estimated from an  $O_2$  profile should be verified against an independent technique. In this study, a hyperbolic tangent model better described the concentration profile, compared to the linear and logarithmic models and yielded values of  $O_2$  flux that were most consistent with the independent technique (i.e., an integrative measure obtained in a stirred chamber). The empirical technique demonstrated in this study determines  $O_2$  flux directly from measured  $O_2$  profiles does not require estimates of flow characteristics (e.g., shear velocity) and can be also used to determine the properties of the bulk  $O_2$  concentration. Moreover, the evaluation of these models using published data from a variety of ecological systems provides consistent results with those obtained for  $O_2$  flux. The determination of mass transfer in the CBL through the analysis of the concentration gradient requires the use of an appropriate model (i.e., hyperbolic tangent model), which includes both diffusive and advective processes and considers the biology and chemistry of the system being investigated.

## References

- Abramoff, M. D., P. J. Magelhaes, and S. J. Ram. 2004. Image processing with ImageJ. *Biophot. Int.* 11:36-42.
- Acrivos, A., and P. L. Chambré. 1957. Laminar boundary layer flows with surface reactions. *Ind. Eng. Chem.* 49:1025-1029.
- Basmadjian, D. 2003. Mass transfer: principles and applications. CRC Press.
- Bird, R. B., W. E. Stewart, and E. N. Lightfoot. 2002. Transport phenomena, 2nd ed. Wiley.
- Chambré, P. L., and O. D. Young. 1958. On the diffusion of chemically reacting species in a laminar boundary layer flow. *Phys. Fluids* 1:48-54.
- Crank, J. 1977. The mathematics of diffusion, 2nd ed. Oxford Univ. Press.
- Cussler, E. L. 1997. Diffusion: Mass transfer in fluid systems, 2nd ed. Cambridge Univ. Press.
- Dade, W. B. 1993. Near-bed turbulence and hydrodynamic control of diffusional mass transfer at the sea floor. *Limnol. Oceanogr.* 50:246-254.
- Dang, V. D. 1983. Steady-state mass transfer with homogeneous and heterogeneous reactions. *AiChE J.* 29:19-25.
- Falter, J. L., M. J. Atkinson, and M. A. Merrifield. 2004. Mass-transfer limitation of nutrient uptake by a wave-dominated reef flat community. *Limnol. Oceanogr.* 49:1820-1831.
- Glud, R. N., J. K. Gundersen, N. P. Revsbech, and B. B. Jørgensen. 1994. Effects on the benthic diffusive boundary layer imposed by microelectrodes. *Limnol. Oceanogr.* 39:462-467.
- Hondzo, M., T. Feyaerts, R. Donovan, and B. L. O'Conner. 2005. Universal scaling of dissolved oxygen distribution at the sediment-water interface: a power law. *Limnol. Oceanogr.* 50:1667-1676.
- Jassby, A. D., and T. Platt. 1976. Mathematical formulation of the relationship between photosynthesis and light for phytoplankton. *Limnol. Oceanogr.* 35:540-547.
- Jørgensen, B. B., and D. J. Des Marais. 1990. The diffusive boundary layer of sediments: Oxygen microgradients over microbial mat. *Limnol. Oceanogr.* 35:1343-1355.
- Kader, B. A. 1981. Temperature and concentration profiles in fully turbulent boundary layers. *Int. J. Heat Mass Transfer* 24:1541-1544.
- Larned, S. T., V. I. Nikora, and B. J. F. Biggs. 2004. Mass-transfer-limited nitrogen and phosphorus uptake by stream periphyton: a conceptual model and experimental evidence. *Limnol. Oceanogr.* 49:1992-2000.
- Larkum, A. W. D., E.-M. Koch, and M. Kühl. 2003. Diffusive boundary layers and photosynthesis of the epilithic algal community of coral reefs. *Mar. Biol.* 142:1073-1082.
- Levich, V. G. 1962. Physicochemical hydrodynamics. Prentice Hall.
- Lewandowski, Z., S. A. Altobelli, and E. Fukushima. 1993. NMR and microelectrode studies of hydrodynamics and kinetics in biofilms. *Biotechnol. Prog.* 9:40-45.
- Lin, C. S., R. W. Moulton, and G. L. Putnam. 1953. Mass transfer between solid wall and fluid streams. *Ind. Eng. Chem.* 45:636-640.
- Lorenzen, J., R. N. Glud, and N. P. Revsbech. 1995. Impact of microsensor-caused changes in diffusive boundary layer thickness on O<sub>2</sub> profiles and photosynthetic rates in benthic communities of microorganisms. *Mar. Ecol. Prog. Ser.* 119:237-241.
- Lorke, A., B. Müller, M. Maerki, and A. Wüest. 2003. Breathing sediments: The control of diffusive transport across the sediment-water interface by periodic boundary-layer turbulence. *Limnol. Oceanogr.* 48:2077-2085.
- Mitrovic, B. M., and D. V. Papavassiliou. 2004. Effects of a first-order chemical reaction on turbulent mass transfer. *Int. J. Heat Mass Transfer* 47:43-61.
- Moore, P., and J. Crimaldi. 2004. Odor landscapes and animal behavior: tracking odor plumes in different physical worlds. *J. Mar. Sci.* 49:55-64.
- Na, Y., and T. J. Hanratty. 2000. Limiting behaviour of turbulent scalar transport close to a wall. *Int. J. Heat Mass Transfer* 43:1749-1758.
- Nishihara, G.-N., and J. D. Ackerman. 2006. The effect of hydrodynamics on the mass transfer of dissolved inorganic carbon to the freshwater macrophyte *Vallisneria spiralis*. *Limnol. Oceanogr.* 51:2734-2735.
- Ploug, H., W. Stolte, E. H. G. Epping, and B. B. Jørgensen. 1999. Diffusive boundary layers, photosynthesis, and respiration of the colony-forming plankton algae, *Phaeocystis* sp. *Limnol. Oceanogr.* 44:1949-1958.
- Rasmussen, K., and Z. Lewandowski. 1998. The accuracy of oxygen flux measurements using microelectrodes. *Wat. Res.* 32:3747-3755.
- Sanford, L. P., and S. M. Crawford. 2000. Mass transfer versus kinetic control of uptake across solid-water boundaries. *Limnol. Oceanogr.* 45:1180-1186.
- Schlichting, H., and K. Gersten. 2000. Boundary-layer theory, 8th ed. Springer.
- Shaw, D. A., and T. J. Hanratty. 1977. Turbulent mass transfer rate to a wall for large Schmidt numbers. *AiChE J.* 23:28-37.
- Stewart, H. L., and R. C. Carpenter. 2003. The effects of morphology and water flow on photosynthesis of marine macroalgae. *Ecology* 84:2999-3012.
- Tennekes, H., and J. L. Lumley. 1972. A first course in turbulence. The MIT Press.
- Thomas, F. I. M., and M. J. Atkinson. 1997. Ammonium uptake by coral reefs: Effects of water velocity and surface roughness on mass transfer. *Limnol. Oceanogr.* 42:81-88.
- Wheeler, W. N. 1980. Effect of boundary layer transport on the fixation of carbon by the giant kelp *Macrocystis pyrifera*. *Mar. Biol.* 56:103-110.
- Wolf-Gladrow, D. and U. Riebesell. 1997. Diffusion and reactions in the vicinity of plankton: a refined model for inorganic carbon transport. *Mar. Chem.* 59:17-34.

Submitted 8 December 2005

Revised 20 April 2006

Accepted 22 August 2006